Adaptive Wideband Beamforming With Frequency Invariance Constraints

Yong Zhao, Wei Liu, *Senior Member, IEEE*, and Richard J. Langley, *Member, IEEE*

***Abstract*—A response variation (RV) element is introduced to control the consistency of an adaptive wideband beamformer's response over the frequency range of interest. By incorporating the RV element into the linearly constrained minimum variance (LCMV) beamformer, we develop a novel linearly constrained beamformer with an improved output signal-to-interference-plus-noise ratio (SINR), compared to both the traditional formulation and the eigenvector based formulation, due to an increased number of degrees of freedom for interference suppression. In addition, two novel wideband beamformers robust against look direction estimation errors are also proposed as a further application of the RV element. One is designed by imposing a constraint on the RV element and simultaneously limiting the magnitude response of the beamformer within a pre-defined angle range at a reference frequency; the other one is obtained by combining the RV element and the worst-case performance optimization method. Both of them are reformulated in a convex form as the second-order cone (SOC) programming problem and solved efficiently using interior point method. Compared with the original robust methods, a more efficient and effective control over the beamformer's response at the look direction region is achieved with an improved overall performance.**

***Index Terms*—Convex optimization, frequency invariance, look direction error, robust beamformer, wideband beamforming.**

I. Introduction

In adaptive wideband beamforming [1], given the direction of arrival (DOA) information of the signal of interest, many traditional beamforming techniques can work effectively and achieve a satisfactory output signal-to-interference-plus-noise ratio (SINR) [2], [3]. One of the most well-known beamformers is the linearly constrained minimum variance (LCMV) beamformer or the Frost beamformer [4], [5], which minimizes its output power while preserving a unity gain at the look direction or subject to some more complicated constraints. Suppose the signal of interest comes from the broadside of the array, then a simple formulation of the constraints can be obtained. However, the problem with this simple formulation is that the beamformer will be over-constrained when we are not interested in the full range of normalized frequency. Moreover, we may not need to constrain the beamformer response over the frequency range of interest to be exactly unity and some variation can be allowed so that more freedom can be allocated for suppressing interferences.

To design a wideband beamformer over a specified frequency range, conventionally we formulate a constraint matrix by sampling the frequency range of interest and constrain the response of the beamformer at those frequency points to be the desired ones. However, the large number of constraints resulted from this approach reduces the number of degrees of freedom in minimizing the output power of the beamformer. To reduce the number of constraints, an eigenvector constraint approach was developed based on the low rank representation of wideband signals [6].

To have a more efficient use of the degrees of freedom of the array, we propose a new method for wideband minimum variance beamforming, with a much less number of constraints, and resulting in a higher output SINR. In this method, a response variation (RV) element will be introduced to control the frequency response of the beamformer at the look direction. Based on the new formulation, an online LMS-type (least mean square) adaptive solution is then derived.

The performance of the above beamformers is very sensitive to array calibration errors, and especially the error in the DOA angle of the signal of interest. If the desired signal does not come exactly from the designed look direction, it will be considered as an interference and the beamformer will tend to null out the desired signal at its output.

Many methods have been proposed to improve the robustness of the beamformer against DOA angle mismatch error [7], [8]. For example, we can impose additional derivative constraints to the beamformer so that a wider main beam can be obtained to cover all the possible directions of the signal of interest [9]–[11]. Another choice is the diagonal loading method which improves the robustness of the beamformer by constraining the norm of its weight vector [8], [12].

Moreover, we can employ inequality constraints to control the magnitude response of the beamformer over a specified DOA range. Such an idea was initially proposed for robust narrowband beamforming [13]–[15]. In this paper, we will extend it to the wideband case and design a robust wideband beamformer based on convex optimization. In the proposed method, the RV element is first constrained to attain a frequency invariant main beam, after which we only need to impose one single soft magnitude constraint at each sampled angle point.

A class of robust beamformers based on worst-case performance optimization using convex optimization techniques have also been proposed for both narrowband and wideband arrays [15]–[17]. In [17], a group of constraints are imposed on sampled frequency points over the frequency range of interest to

Manuscript received June 15, 2010; revised August 17, 2010; accepted September 16, 2010. Date of publication February 04, 2011; date of current version April 06, 2011.

The authors are with Communications Research Group, Department of Electronic & Electrical Engineering, University of Sheffield, Sheffield S1 3JD, U.K. (e-mail: yong.zhao@sheffield.ac.uk; w.liu@sheffield.ac.uk; r.j.langley@sheffield.ac.uk).

Digital Object Identifier 10.1109/TAP.2011.2110630

prevent the mismatched desired signal from being filtered out by the beamformer. There are two problems with the approach. One is its relatively high computational complexity due to its constraints imposed on a large number of sampled frequency points; the other one is that there is no mechanism to control the response consistency to the mismatched desired signal so that a potentially intolerable distortion to the desired signal may happen. To address the above two problems, we first apply the RV element to the array to ensure a good response consistency in the robust DOA region, and then impose just one constraint on the reference frequency point at the look direction. Compared to the approach in [17], both the system's efficiency and the frequency response consistency to the desired signal are improved significantly.

This paper is organized as follows. The wideband beamforming structure with tapped delay-lines (TDLs) is reviewed briefly in Section II, including the Frost beamformer with its two solutions. The traditional adaptive wideband beamformer with added frequency invariance constraints is proposed in Section III. The two wideband beamformers robust against look direction estimation errors are proposed in Section IV. Simulation results are provided in Section V, where the performances of both the proposed methods and the conventional methods are compared in details. Conclusions are drawn in Section VI.

II. Wideband Beamforming

A general structure for wideband beamforming is shown in Fig. 1, where J is the number of taps associated with each of the M sensor channels. The beamformer obeying this architecture samples the propagating wave field in both space and time. Its response as a function of the angular frequency ω and DOA θ can be expressed as

$$\tilde{R}(\omega,\theta)=\sum_{m=0}^{M-1}\sum_{k=0}^{J-1}w_{m,k}e^{-j\omega(\tau_m+kT_s)} \tag{1}$$

where T_s is the unit delay in the TDL or sampling period, τ_m is the delay between the mth sensor and the zero-phase reference point. In a vector form, we have

$$\tilde{R}(\omega,\theta)=\mathbf{w}^T\mathbf{s}(\omega,\theta) \tag{2}$$

where $\mathbf{w}$ is the coefficient vector defined as

$$\mathbf{w}=[w_{0,0},\cdots,w_{M-1,0},\cdots,w_{0,J-1},\cdots,w_{M-1,J-1}]^T \tag{3}$$

and $\mathbf{s}(\omega,\theta)$ is the $MJ\times 1$ steering vector given by

$$\mathbf{s}(\omega,\theta)=\left[e^{-j\omega\tau_0},\cdots,e^{-j\omega\tau_{M-1}},\cdots,e^{-j\omega(\tau_0+(J-1)T_s)},\cdots,e^{-j\omega(\tau_{M-1}+(J-1)T_s)}\right]^T. \tag{4}$$

For a uniform linear array (ULA) with an inter-element spacing d, $\tau_m=\tau_0+m(d/c)\sin\theta$. With the normalized angular frequency $\Omega=\omega T_s$, we have

$$\Delta_{m,k}=\omega(\tau_m+kT_s)=\Omega(\tau_0/T_s+m\mu\sin\theta+k) \tag{5}$$

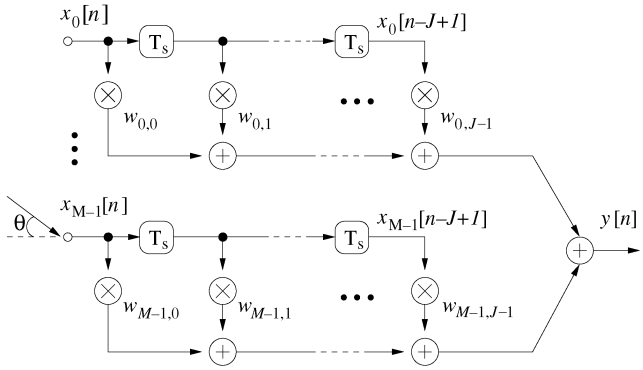

Fig. 1. A general wideband beamforming structure.

with $\mu=d/cT_s$. Then we obtain the response as a function of Ω and θ

$$R(\Omega,\theta)=\mathbf{w}^T\mathbf{s}(\Omega,\theta) \tag{6}$$

with

$$\mathbf{s}(\Omega,\theta)=[e^{-j\Omega\Delta_{0,0}},\cdots,e^{-j\Omega\Delta_{M-1,0}},\cdots,e^{-j\Omega\Delta_{0,J-1}},\cdots,e^{-j\Omega\Delta_{M-1,J-1}}]^T. \tag{7}$$

In our simulations,we choose the middle point of the array as the zero-phase reference point so that $\tau_0=-(J-1)T_s/2$.

Suppose the signal of interest comes from the broadside of the array ($\theta=0$). Then the Frost beamformer can be formulated as follows:

$$\min\quad \mathbf{w}^T\mathbf{R}_{xx}\mathbf{w}\ \text{subject to}\quad \mathbf{C}^T\mathbf{w}=\mathbf{f} \tag{8}$$

where $\mathbf{R}_{xx}=E\{\mathbf{x}[n]\mathbf{x}[n]^T\}$ is the covariance matrix of the received array signal with

$$\mathbf{x}(n)=[x_0[n],\cdots,x_{M-1}[n],\cdots,x_0[n-J+1],\cdots,x_{M-1}[n-J+1]]^T \tag{9}$$

and $\mathbf{C}$ is a $MJ\times J$ constraint matrix

$$\mathbf{C}=\begin{pmatrix}\mathbf{1}_M & \mathbf{0}_M & \cdots & \mathbf{0}_M\\ \mathbf{0}_M & \mathbf{1}_M & \cdots & \mathbf{0}_M\\ \vdots & \vdots & \ddots & \vdots\\ \mathbf{0}_M & \mathbf{0}_M & \cdots & \mathbf{1}_M\end{pmatrix} \tag{10}$$

where $\mathbf{1}_M$ and $\mathbf{0}_M$ are the $M\times 1$ column vectors containing ones and zeros, respectively. $\mathbf{f}$ is the $J\times 1$ response vector with one entry being 1 and all the others being zero.

The solution to the problem in (8) can be obtained by the method of Lagrange multipliers, given by [4]

$$\mathbf{w}_{opt}=\mathbf{R}_{xx}^{-1}\mathbf{C}\left(\mathbf{C}^T\mathbf{R}_{xx}^{-1}\mathbf{C}\right)^{-1}\mathbf{f} \tag{11}$$

where $\mathbf{R}_{xx}$ can be approximated by the sample covariance matrix $\hat{\mathbf{R}}_{xx}$

$$\hat{\mathbf{R}}_{xx}=\frac{1}{K}\sum_{n=0}^{K-1}\mathbf{x}[n]\mathbf{x}[n]^T \tag{12}$$

with K being the number of samples available.

Alternatively, an online LMS-type solution to the problem in (8) can be obtained as [4]

$$\mathbf{w}[n+1] = \mathbf{w}[0] + \mathbf{P}\left(\mathbf{w}[n] - \mu e[n]\mathbf{x}[n]\right) \tag{13}$$

with

$$\begin{aligned}\mathbf{w}[0] &= \mathbf{C}(\mathbf{C}^T\mathbf{C})^{-1}\mathbf{f}, \quad \mathbf{P} = \mathbf{I} - \mathbf{C}(\mathbf{C}^T\mathbf{C})^{-1}\mathbf{C}^T \\ e[n] &= y[n] = \mathbf{w}[n]^T\mathbf{x}[n]\end{aligned} \tag{14}$$

where μ is a real-valued step size.

III. Adaptive Wideband Beamformer With Frequency Invariance Constraints

Given the constraints of the Frost beamformer in (8), the unity gain is preserved at the broadside direction over all possible frequencies. However, in many cases, the frequency range of interest is not the entire normalized frequency band and it is not necessary to maintain an exact unity gain over the frequency range of interest either. Applying the constraints only to the frequency range of interest and simultaneously reducing the consistency of the beamformer's response at the look direction over the operating frequency range will leave more degrees of freedom for the beamformer to suppress the interfering signals.

To design a wideband beamformer with a specified frequency range, conventionally we can formulate the constraint matrix by sampling the frequency range of interest and constrain the response of the beamformer to those frequency points to be the desired ones, which are usually some pure delays or zeros if we want to null out this signal. In this case broadside arrival of the signal of interest is unnecessary so that θ can be any angle within $[-90^\circ, 90^\circ]$ (for a linear array). Suppose the frequency range of interest is Ω_I and we uniformly sample Ω_I with $\hat{r}$ frequency points Ω_i, $i = 0, 1, \cdots, \hat{r} - 1$. The corresponding desired response of the beamformer for the frequency point Ω_i with the direction θ is given by $D(\Omega_i, \theta)$. Then the constraint for the $\hat{r}$ frequency points can be formulated as

$$\mathbf{S}^T\mathbf{w} = \mathbf{g} \tag{15}$$

where $\mathbf{S}$ is an $MJ \times \hat{r}$ constraint matrix

$$\mathbf{S} = [\mathbf{s}(\Omega_0, \theta), \mathbf{s}(\Omega_1, \theta), \cdots, \mathbf{s}(\Omega_{\hat{r}-1}, \theta)] \tag{16}$$

and $\mathbf{g}$ is an $\hat{r} \times 1$ response vector

$$\mathbf{g} = [D(\Omega_0, \theta), D(\Omega_1, \theta), \cdots, D(\Omega_{\hat{r}-1}, \theta)]^T. \tag{17}$$

Note that $\mathbf{S}$ and $\mathbf{g}$ are complex-valued and we can change the complex constraints into real ones as follows (for a real-valued $\mathbf{w}$)

$$\hat{\mathbf{S}}^T\mathbf{w} = \hat{\mathbf{g}} \tag{18}$$

with

$$\begin{aligned}\hat{\mathbf{S}} = [&\Re\{\mathbf{s}(\Omega_0, \theta)\}, \Im\{\mathbf{s}(\Omega_0, \theta)\}, \cdots, \\ &\Re\{\mathbf{s}(\Omega_{\hat{r}-1}, \theta)\}, \Im\{\mathbf{s}(\Omega_{\hat{r}-1}, \theta)\}] \\ \hat{\mathbf{g}} = [&\Re\{D(\Omega_0, \theta)\}, \Im\{D(\Omega_0, \theta)\}, \cdots, \\ &\Re\{D(\Omega_{\hat{r}-1}, \theta)\}, \Im\{D(\Omega_{\hat{r}-1}, \theta)\}]^T\end{aligned} \tag{19}$$

where $\Re\{\bullet\}$ and $\Im\{\bullet\}$ denote the real part and imaginary part of their variables, respectively.

Note that the constraints are assumed to be linearly independent so that $\hat{\mathbf{S}}$ has a rank $\hat{r}$. This is not an efficient way to utilize the degrees of freedom of the array, since each linear constraint uses one degree of freedom in the weight vector $\mathbf{w}$. With $2\hat{r}$ constraints there are only $ML - 2\hat{r}$ degrees of freedom available for minimizing the output power of the array.

A more efficient representation is the eigenvector constraint design approach developed based on the low-rank representation of wideband source signals with singular value decomposition (SVD) [6]. As shown in Appendix I, the constraints in (18) can be approximated by

$$\mathbf{U}_r^T\mathbf{w} = \hat{\mathbf{g}}_r. \tag{20}$$

Combining the eigenvector constraints in (20) along with the minimization of output power of the beamformer, we have the following new LCMV formulation

$$\min \quad \mathbf{w}^T\mathbf{R}_{xx}\mathbf{w} \quad \text{subject to} \quad \mathbf{U}_r^T\mathbf{w} = \hat{\mathbf{g}}_r \tag{21}$$

with its LMS-type solution as

$$\mathbf{w}[n+1] = \mathbf{w}[0] + \mathbf{P}\left(\mathbf{w}[n] - \mu e[n]\mathbf{x}[n]\right) \tag{22}$$

where

$$\mathbf{w}[0] = \mathbf{U}_r\left(\mathbf{U}_r^T\mathbf{U}_r\right)^{-1}\hat{\mathbf{g}}, \quad \mathbf{P} = \mathbf{I} - \mathbf{U}_r\left(\mathbf{U}_r^T\mathbf{U}_r\right)^{-1}\mathbf{U}_r^T. \tag{23}$$

By (20), the number of constraints is reduced compared to that in (18), However as shown in Appendix II, when both the frequency range of interest and the dimension of the array is large, this approach still leads to a large number of constraints. Furthermore, these constraints are "hard" and each of them will take exactly one degree of freedom from the system. In the next, we propose a "soft" approach to the design of constraints by introducing a new element to control the beamformer's response over the frequency range of interest at the look direction, which is called response variation (RV). In a general form, it is defined as [18]–[20]

$$\begin{aligned}RV &= \int_{\Omega_I}\int_{\Theta_{FI}} \left|\mathbf{w}^T\mathbf{s}(\Omega, \theta) - \mathbf{w}^T\mathbf{s}(\Omega_r, \theta)\right|^2 d\Omega d\theta \\ &= \mathbf{w}^T\mathbf{Q}\mathbf{w} \quad \text{with}\end{aligned} \tag{24}$$

$$\begin{aligned}\mathbf{Q} = \int_{\Omega_I}\int_{\Theta_{FI}} &\Re\{(\mathbf{s}(\Omega, \theta) - \mathbf{s}(\Omega_r, \theta) \\ &\times \left(\mathbf{s}(\Omega, \theta) - \mathbf{s}(\Omega_r, \theta)^H\right\} d\Omega d\theta\end{aligned} \tag{25}$$

where Θ_{FI} shows the DOA range over which the RV parameter is measured, Ω_r is the reference frequency and we have assumed that $\mathbf{w}$ is real-valued. RV is a measurement of the Euclidean distance between the response at Ω_r and that at all the other operating frequencies over a range of directions over which the RV is measured. When RV is zero, the beamformer has a consistent frequency invariant response over the frequency range Ω_I and the DOA range Θ_{FI}.

Since we only consider the look direction θ_0, Θ_{FI} is reduced to a single DOA angle point. Then (24) and (25) change to

$$RV_0 = \int_{\Omega_I} \left|\mathbf{w}^T\mathbf{s}(\Omega,\theta_0) - \mathbf{w}^T\mathbf{s}(\Omega_r,\theta_0)\right|^2 d\Omega = \mathbf{w}^T\mathbf{Q}_0\mathbf{w} \tag{26}$$

and

$$\mathbf{Q}_0 = \int_{\Omega_I} \Re\left\{(\mathbf{s}(\Omega,\theta_0) - \mathbf{s}(\Omega_r,\theta_0) \times \left(\mathbf{s}(\Omega,\theta_0) - \mathbf{s}(\Omega_r,\theta_0)^H\right\} d\Omega \tag{27}$$

respectively.

In the simulation, $\mathbf{Q}_0$ is calculated numerically by uniformly discretizing Ω_I into N_f grid points. To control the consistency of the frequency response of the beamformer at θ_0 and also make sure the beamformer reaches the desired response, we can minimize RV_0 and simultaneously constrain the beamformer's response at (Ω_r,θ_0) to the desired response $D(\Omega_r,\theta_0)$, given by

$$\mathbf{s}(\Omega_r,\theta_0)^T\mathbf{w} = D(\Omega_r,\theta_0). \tag{28}$$

Then the complete formulation for the proposed minimum variance beamformer can be obtained by combining (26) and (28) along with minimizing output power of the beamformer

$$\begin{aligned} \min \quad & \mathbf{w}^T(\mathbf{R}_{xx} + \beta\mathbf{Q}_0)\mathbf{w} \\ \text{subject to} \quad & \mathbf{s}(\Omega_r,\theta_0)^T\mathbf{w} = D(\Omega_r,\theta_0) \end{aligned} \tag{29}$$

where β is a real-valued trade-off parameter between the frequency invariant property at the look direction and the output power of the beamformer. A large β will increase the consistency of the resultant beamformer's response over the frequency range of interest at the look direction.

Note that the constraint in (28) is complex-valued and we can change the single complex constraint into two real ones as follows:

$$\tilde{\mathbf{C}}^T\mathbf{w} = \tilde{\mathbf{f}} \tag{30}$$

with

$$\begin{aligned} \tilde{\mathbf{C}} &= \left[\Re\left\{\mathbf{s}(\Omega_r,\theta_0)\right\}, \Im\left\{\mathbf{s}(\Omega_r,\theta_0)\right\}\right] \\ \tilde{\mathbf{f}} &= \left[\Re\left\{D(\Omega_r,\theta_0)\right\}, \Im\left\{D(\Omega_r,\theta_0)\right\}\right]^T. \end{aligned} \tag{31}$$

Then we can change (29) to

$$\begin{aligned} \min \quad & \mathbf{w}^T(\mathbf{R}_{xx} + \beta\mathbf{Q}_0)\mathbf{w} \\ \text{subject to} \quad & \tilde{\mathbf{C}}^T\mathbf{w} = \tilde{\mathbf{f}}. \end{aligned} \tag{32}$$

Similar to the Frost beamformer in (13), we can easily derive an online LMS-type algorithm for the new problem in (32), as given in the following:

$$\mathbf{w}[n+1] = \mathbf{w}[0] + \mathbf{P}\left\{\mathbf{w}[n] - \mu\left(e[n]\mathbf{x}[n] + \beta\mathbf{Q}_0\mathbf{w}[n]\right)\right\} \tag{33}$$

with

$$\mathbf{w}[0] = \tilde{\mathbf{C}}(\tilde{\mathbf{C}}^T\tilde{\mathbf{C}})^{-1}\tilde{\mathbf{f}}, \quad \mathbf{P} = \mathbf{I} - \tilde{\mathbf{C}}(\tilde{\mathbf{C}}^T\tilde{\mathbf{C}})^{-1}\tilde{\mathbf{C}}^T. \tag{34}$$

Compared to the eigenvector constraint approach in (21), the number of 'hard' constraints is reduced significantly to only two and the consistency of the beamformer's response at the look direction is represented by part of the cost function to be minimized. Thus the output SINR is expected to be improved due to the reduced number of 'hard' constraints.

IV. Robust Wideband Beamformer Against Look Direction Estimation Error

When the desired signal does not come exactly from the designed look direction θ_0, the beamformer will tend to suppress it as an interference. All the approaches introduced in the last section are very sensitive to this error. To improve the robustness of the system against the look direction estimation error, we next propose two methods based on convex optimization.

A. Robust Wideband Beamformer With Frequency Invariance Constraints

The first approach is based on a previously proposed method for robust narrowband beamforming, where inequality constraints on the magnitude response of the beamformer over a specified DOA range were introduced [13]–[15]

$$\delta_l \le |G(\theta)| \le \delta_u, \theta \in [\theta_l,\theta_u] \tag{35}$$

where $G(\theta)$ is the response of a narrowband beamformer, δ_l and δ_u are the lower and upper limits of the magnitude response, and $[\theta_l,\theta_u]$ is the DOA range where the magnitude constraints are imposed. This idea can be extended to the wideband case directly as follows:

$$\delta_l \le |R(\Omega,\theta)| \le \delta_u, \theta \in [\theta_l,\theta_u], \quad \Omega \in \Omega_I. \tag{36}$$

To represent the frequency-angle constraints in (36), we have to sample both the angle and the frequency ranges by a sufficiently large number of points. Although we can employ the approach in (20) for a more effective representation, it still demands a large number of constraints over the DOA range. An efficient solution is to incorporate the RV element into the constraint set to achieve a frequency invariant main beam so that we only need to impose one magnitude constraint at each sampled angle point corresponding to the reference frequency Ω_r.

We first limit the RV element in (24) to a very small value σ^2 by imposing the following constraint:

$$RV \le \sigma^2 \tag{37}$$

which can be simplified into

$$RV = \left\|\mathbf{L}_1^T\mathbf{w}\right\|_2^2 \le \sigma^2 \tag{38}$$

where $\mathbf{L}_1 = \mathbf{V}_1\mathbf{U}_1^{1/2}$, with $\mathbf{U}_1$ being a diagonal matrix including all the eigenvalues of $\mathbf{Q}$, and $\mathbf{V}_1$ being the eigenvector matrix containing the corresponding eigenvectors. Note here RV is calculated for the range $\Theta_{FI} = [\theta_l,\theta_u]$. In the simulation, $\mathbf{Q}$ is computed numerically and Ω_I and $\Theta_{FI} = [\theta_l,\theta_u]$ are uniformly discretized into N_f and N_θ grid points, respectively.

With this constraint, we now only need to impose the magnitude constraints at Ω_r, given by

$$\delta_l \le |R(\Omega_r,\theta)| \le \delta_u, \quad \theta \in [\theta_l,\theta_u]. \tag{39}$$

Note that the formulation in (39) is not convex due to the part $|R(\Omega_r,\theta)| \ge \delta_l$. To convert it into a convex form, as an approximation, we use

$$\Re\{R(\Omega_r,\theta)\} \ge \delta_l. \tag{40}$$

Similarly we have

$$\mathbf{w}^T\mathbf{R}_{xx}\mathbf{w} = \left\|\mathbf{L}_2^T\mathbf{w}\right\|_2^2 \tag{41}$$

where $\mathbf{L}_2 = \mathbf{V}_2\mathbf{U}_2^{1/2}$, with $\mathbf{U}_2$ being the diagonal matrix including all the eigenvalues of $\mathbf{R}_{xx}$, and $\mathbf{V}_2$ being the corresponding eigenvector matrix.

To avoid a large noise gain, we also need to constrain the norm of $\mathbf{w}$ [21]

$$\|\mathbf{w}\|_2 < \chi \tag{42}$$

where χ is a positive real-valued constant.

Then, a complete formulation for the first robust wideband beamformer with a frequency invariance constraint (RB-FI) is obtained as

$$\begin{aligned} \min \quad & \left\|\mathbf{L}_2^T\mathbf{w}\right\|_2 \\ \text{subject to} \quad & \left\|\mathbf{L}_1^T\mathbf{w}\right\|_2 \le \sigma; \quad \left|\mathbf{w}^T\mathbf{s}(\Omega_r,\theta)\right| \le \delta_u \\ & \Re\left\{\mathbf{w}^T\mathbf{s}(\Omega_r,\theta)\right\} \ge \delta_l, \quad \theta \in [\theta_l,\theta_u] \\ & \|\mathbf{w}\|_2 < \chi. \end{aligned} \tag{43}$$

B. Robust Wideband Beamformer With Frequency Invariance Constraints and the Worst-Case Performance Optimization

In this section, we will propose another wideband beamformer robust against the look direction estimation error based on the worst-case performance optimization.

In the presence of look direction estimation error, the actual steering vector differs from the ideal one by an error vector $\mathbf{e}_{s0}(\Omega)$

$$\hat{\mathbf{s}}(\Omega,\theta_s) = \mathbf{s}(\Omega,\theta_0) + \mathbf{e}_{s0}(\Omega), \quad \Omega \in \Omega_I \tag{44}$$

where $\hat{\mathbf{s}}(\Omega,\theta_s)$ is the real steering vector of the desired signal from direction θ_s, and $\mathbf{s}(\Omega,\theta_0)$ is the steering vector corresponding to the designed look direction θ_0.

The worst-case performance optimization approach tries to eliminate the uncertainty included in the steering vector by upper bounding the norm of the error vector $\mathbf{e}_{s0}(\Omega)$, given by

$$\|\mathbf{e}_{s0}(\Omega)\|_2 \le \epsilon, \quad \Omega \in \Omega_I \tag{45}$$

where ϵ is a small positive value.

In [17], a robust wideband beamforming design method based on the worst-case performance optimization (RB-WC) has been proposed with the following formulation

$$\begin{aligned} \min \quad & \mathbf{w}^T\mathbf{R}_{xx}\mathbf{w} \\ \text{subject to} \quad & \Re\left\{\mathbf{w}^T\hat{\mathbf{s}}(\Omega,\theta_s)\right\} \ge 1, \quad \Omega \in \Omega_I. \end{aligned} \tag{46}$$

Then the constraint in (46) can be rewritten as

$$\begin{aligned} \Re\left\{\mathbf{w}^T\hat{\mathbf{s}}(\Omega,\theta_s)\right\} &= \mathbf{w}^T\Re\left\{\hat{\mathbf{s}}(\Omega,\theta_s)\right\} \\ &= \mathbf{w}^T\Re\left\{\mathbf{s}(\Omega,\theta_0) + \mathbf{e}_{s0}(\Omega)\right\} \\ &= \mathbf{w}^T\Re\left\{\mathbf{s}(\Omega,\theta_0)\right\} + \mathbf{w}^T\Re\left\{\mathbf{e}_{s0}(\Omega)\right\}. \end{aligned} \tag{47}$$

Applying the Cauchy-Schwartz inequalities along with the inequality $\|\mathbf{e}_{s0}(\Omega)\|_2 \le \epsilon, \Omega \in \Omega_I$, we have

$$\begin{aligned} \Re\left\{\mathbf{w}^T\hat{\mathbf{s}}(\Omega,\theta_s)\right\} &\ge \mathbf{w}^T\Re\left\{\mathbf{s}(\Omega,\theta_0)\right\} - \|\mathbf{w}\|_2\left\|\Re\left\{\mathbf{e}_{s0}(\Omega)\right\}\right\|_2 \\ &\ge \mathbf{w}^T\Re\left\{\mathbf{s}(\Omega,\theta_0)\right\} - \epsilon\|\mathbf{w}\|_2. \end{aligned} \tag{48}$$

Thus, to satisfy the constraint in (46), we can let

$$\mathbf{w}^T\Re\left\{\mathbf{s}(\Omega,\theta_0)\right\} - \epsilon\|\mathbf{w}\|_2 \ge 1 \tag{49}$$

$$\Leftrightarrow \epsilon\|\mathbf{w}\|_2 \le \mathbf{w}^T\Re\left\{\mathbf{s}(\Omega,\theta_0)\right\} - 1. \tag{50}$$

Then the RB-WC problem in (46) changes to

$$\begin{aligned} \min \quad & \left\|\mathbf{L}_2^T\mathbf{w}\right\|_2 \\ \text{subject to} \quad & \epsilon\|\mathbf{w}\|_2 \le \mathbf{w}^T\Re\left\{\mathbf{s}(\Omega,\theta_0)\right\} - 1, \quad \Omega \in \Omega_I. \end{aligned} \tag{51}$$

A potential problem with the above method is that the magnitude response of the resultant beamformer at the desired direction can vary for different frequencies and this kind of variation could be out of control and cause very large distortions to the desired signal. Moreover, as in the previous case, we also need to sample the frequency range of interest by a sufficiently large number of points, which will inevitably increase the computational complexity of the system. As a remedy, we can apply the RV constraint in the same way as before, which will improve the frequency invariance property of the resultant beamformer at the desired direction and also reduce the computational complexity of the system. In this case the RV constraint is given by

$$RV = \left\|\mathbf{L}_1^T\mathbf{w}\right\|_2^2 \le \varsigma^2 \tag{52}$$

where ς is a small positive value. Then the formulation in (46) can be simplified to

$$\begin{aligned} \min \quad & \mathbf{w}^T\mathbf{R}_{xx}\mathbf{w} \text{ subject to } \quad RV \le \varsigma^2 \\ & \Re\left\{\mathbf{w}^T\hat{\mathbf{s}}(\Omega_r,\theta_s)\right\} \ge 1. \end{aligned} \tag{53}$$

Similarly, the second constraint in (53) can be replaced by

$$\epsilon\|\mathbf{w}\|_2 \le \mathbf{w}^T\Re\left\{\mathbf{s}(\Omega_r,\theta_0)\right\} - 1. \tag{54}$$

Then we obtain the following convex formulation for designing the robust wideband beamformer with the frequency invariance constraints and the worst-case performance optimization (RB-FI-WC)

$$\begin{aligned} \min \quad & \left\|\mathbf{L}_2^T\mathbf{w}\right\|_2 \quad \text{subject to} \quad \left\|\mathbf{L}_1^2\mathbf{w}\right\|_2 \le \varsigma \\ & \epsilon\|\mathbf{w}\|_2 \le \mathbf{w}^T\Re\left\{\mathbf{s}(\Omega_r,\theta_0)\right\} - 1. \end{aligned} \tag{55}$$

Since there are only two constraints imposed in (55), the computational complexity of the system will be reduced significantly compared to the method in (51).

C. Algorithm Implementation

Next we will develop a second-order cone (SOC) formulation of (55) and then solve it using the optimization tool SeDuMi [22]. Following [16], by introducing a new non-negative variable ρ, we let $\|L_2^T\mathbf{w}\|_2 \le \rho$. Equation (55) can be converted to

$$\begin{aligned} \min \quad & \rho \\ \text{subject to} \quad & \left\|\mathbf{L}_2^T\mathbf{w}\right\|_2 \le \rho; \quad \|\mathbf{L}_1\mathbf{w}\|_2 \le \varsigma \\ & \epsilon\|\mathbf{w}\|_2 \le \mathbf{w}^T\Re\left\{\mathbf{s}(\Omega_r,\theta_0)\right\} - 1 \end{aligned} \tag{56}$$

which can be further transformed to the following canonical dual form of the SOC programming problem as

$$\begin{aligned} &\min \quad \mathbf{d}^T\mathbf{y} \quad \text{subject to} \\ &\mathbf{f}+\mathbf{F}^T\mathbf{y} \in \mathrm{SOC}_1^{MJ+1}\times\mathrm{SOC}_2^{MJ+1}\times\mathrm{SOC}_3^{MJ+1} \end{aligned} \tag{57}$$

where $\mathbf{y}$ is the variable vector, SOC_i^{MJ+1} is the quadratic cone of the dimension $MJ+1$ corresponding to the ith inequality constraint in (56) ($i = 1, 2, 3$), and

$$\begin{aligned} \mathbf{d} &= [1, \mathbf{0}^T]^T \in R^{(MJ+1)\times 1} \\ \mathbf{y} &= [\rho, \mathbf{w}^T]^T \in R^{(MJ+1)\times 1} \\ \mathbf{f} &= [\mathbf{0}^T, \varsigma, -1, \mathbf{0}^T]^T \in R^{(3MJ+3)\times 1} \\ \mathbf{F}^T &= \begin{bmatrix} 1 & \mathbf{0}^T \\ \mathbf{0} & \mathbf{L}_2^T \\ 0 & \mathbf{0}^T \\ \mathbf{0} & \mathbf{L}_1^T \\ 0 & \Re\left\{\mathbf{s}(\Omega_r,\theta_0)\right\}^T \\ \mathbf{0} & \epsilon\mathbf{I} \end{bmatrix} \in R^{(3MJ+3)\times(MJ+1)}. \end{aligned} \tag{58}$$

More specifically

$$\mathrm{SOC}_i^{MJ+1} = \left\{\tilde{\mathbf{p}}_i \in R^{MJ+1} | p_i \ge \|\overline{\mathbf{p}}_i\|_2\right\}, \quad i = 1, 2, 3 \tag{59}$$

and

$$\begin{aligned} \mathbf{p} &= \left[\tilde{\mathbf{p}}_1^T, \tilde{\mathbf{p}}_2^T, \tilde{\mathbf{p}}_3^T\right]^T \\ &= \left[\rho, \mathbf{w}^T\mathbf{L}_2, \varsigma, \mathbf{w}^T\mathbf{L}_1, \mathbf{w}^T\Re\left\{\mathbf{s}(\Omega_r,\theta_0)\right\} - 1, \epsilon\mathbf{w}^T\right]^T \\ &= \mathbf{f} + \mathbf{F}^T\mathbf{y} \end{aligned} \tag{60}$$

where

$$\begin{aligned} \tilde{\mathbf{p}}_1 &= [p_1, \overline{\mathbf{p}}_1\}] = [\rho, \mathbf{w}^T\mathbf{L}_2]^T \\ \tilde{\mathbf{p}}_2 &= [p_2, \overline{\mathbf{p}}_2\}] = [\varsigma, \mathbf{w}^T\mathbf{L}_1]^T \\ \tilde{\mathbf{p}}_3 &= [p_3, \overline{\mathbf{p}}_3\}] = \left[\mathbf{w}^T\Re\left\{\mathbf{s}(\Omega_r,\theta_0)\right\} - 1, \epsilon\mathbf{w}^T\right]^T. \end{aligned} \tag{61}$$

Note the only desired weights in $\mathbf{y}$ after optimization is $\mathbf{w}$. The methods in (43) and (51) can be transformed to the canonical dual form of the SOC programming problem in the same way. Using the primal-dual reduction method, the computational complexity of the RB-FI-WC is $O(3^{1.5}M^3J^3)$ and that of the RB-WC is $O(N_f^{1.5}M^3J^3)$ [23]. Since $N_f \gg 3$, our proposed RB-FI-WC has a substantially lower computational complexity than that of RB-WC.

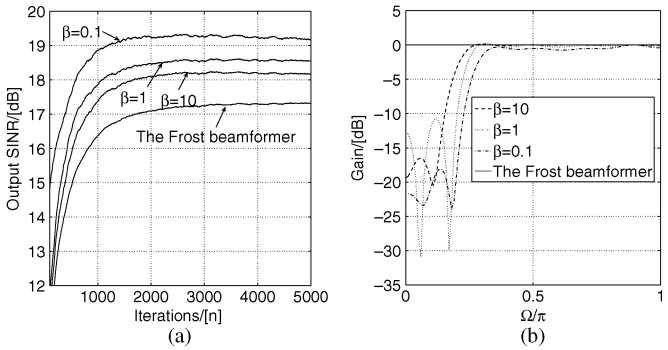

Fig. 2. Comparison of the Frost beamformer in (13) and the RV approach in (33) with $\beta = 10$, 1 and 0.1: (a) convergence of the output SINR; (b) frequency responses at the look direction.

V. Simulations and Results

To show the effectiveness of the proposed methods, simulations are performed based on a ULA with the following specifications.

- We consider a ULA with $M = 10$ and $J = 20$; $\Omega_I = [0.25\pi, \pi]$ and $\Omega_r = 0.25\pi$;
- the array spacing is assumed to be half the wavelength corresponding to the maximum normalized signal frequency π so that $\mu = 1$;
- the desired signal has a signal-to-noise ratio (SNR) of 10 dB and two wideband interferences have a signal-to-interference ratio (SIR) of -10 dB. The directions of arrival for the three signals vary in different design examples;
- desired response $D(\Omega,\theta) = 1$.

A. The LMS-Type Adaptive Beamformers

First we compare the performance of the proposed RV approach in (33) and the LMS-type Frost beamformer in (13). It is assumed that the desired signal comes from the broadside direction and two interferences arrive from the directions $\theta_I = -30°$ and 20°, respectively. The step size μ is set to 0.000004 for both cases and three values of the trade-off parameter β are used with 10, 1 and 0.1, respectively.

Fig. 2(a) shows the learning curves for the output SINR versus the iteration number n for both the Frost beamformer and the proposed one, which is obtained by averaging 200 simulation results. We can see clearly that the proposed RV based one has led to an improved output SINR compared to the Frost beamformer. Moreover, with β decreasing, a higher output SINR has been achieved, which can be explained by the fact that more degrees of freedom are released for interference suppression by relaxing the consistency constraint at the look direction. The resultant frequency responses at the look direction by the Frost beamformer and the proposed one are shown in Fig. 2(b), where we can see that the Frost beamformer has exactly a unity response over all frequency components at the look direction, while with a decreasing β, the frequency response consistency of the proposed RV approach becomes poor, as expected. Next we compare the performances of the proposed RV approach in (33) and the eigenvector constraint approach in (22). Since both can be directly used to design beamformers with an off-broadside main beam, we assume the desired signal comes from $\theta_0 = -30°$

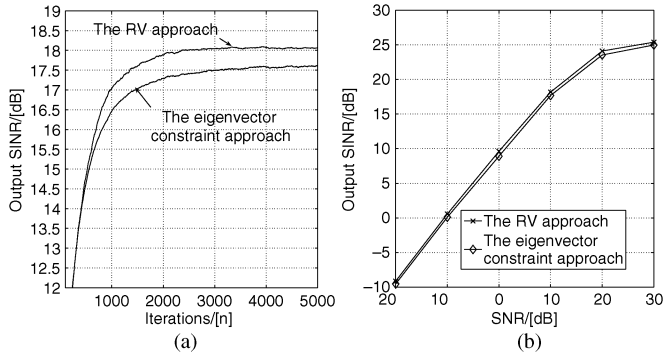

Fig. 3. Comparison of the RV approach in (33) and the eigenvector constraint approach in (22): (a) convergence of the output SINR; (b) output SINR versus input SNR.

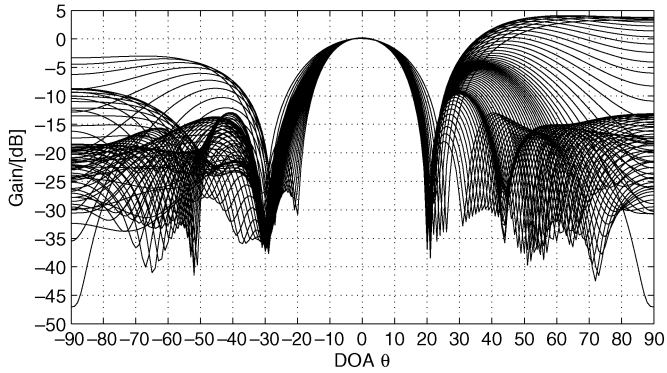

Fig. 4. The resultant beam pattern based on the RB-FI beamformer with the RV constraint applied to $[-10^\circ, 10^\circ]$.

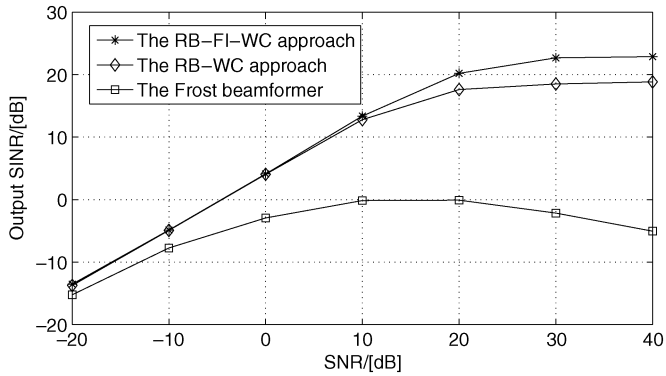

Fig. 5. Output SINR versus input SNR for the RB-FI-WC beamformer, the RB-WC beamformer and the Frost beamformer in (11) with an angle estimation error of 10°.

and the two interferences arrive from $\theta_I = -40^\circ$ and 0°, respectively. The step size μ is set to 0.000004 and 0.000006 for the RV approach and the eigenvector constraint approach, respectively. For the eigenvector constraint approach, as $M = 10$, $J = 20$, $\theta_0 = -30^\circ$ and the frequency range of interest $\Omega_I = [0.25\pi, \pi]$, we have $D_\theta \geq 19$. Therefore, we choose $r = 19$. The learning curves for the output SINR versus the iteration number n are shown in Fig. 3(a), obtained by averaging 200 simulation results. The proposed RV approach achieves a better performance in terms of interference suppression than that of the eigenvector constraint approach. Additionally, in this case the resultant variance of the magnitude responses at the direction $\theta_0 = -30^\circ$ for the proposed RV approach and the eigenvector constraint approach is 0.0084235 and 0.0091174, respectively, which indicates that the former one leads to a slightly better consistency at the look direction than the latter one. Thus we can conclude that the proposed RV approach can achieve an improved performance compared to the eigenvector constraint approach under the condition that they have similar consistency of responses at the look direction. The improvement in performance arises from a larger number of freedom for interference suppression by the RV approach. For this case, the RV approach has $200 - 2 = 198$ degrees of freedom available for minimizing the cost function of the beamformer; in contrast, the eigenvector constraint approach has only $200 - 19 = 181$ degrees of freedom available.

We also give the output SINR result versus the input SNR for both approaches in Fig. 3(b). It can be observed that the RV approach can always achieve a better output SINR for any given value of the input SNR.

B. Robust Beamformers Against Look Direction Error

In this section, we perform simulations for the two proposed robust beamformers: the RB-FI beamformer in (43) and the RB-FI-WC beamformer in (55). In addition, the results based on the previously proposed RB-WC beamformer in (51) and the Frost beamformer with the Lagrange multipliers solution in (11) are also provided as a comparison. The desired signal comes from the direction $\theta_s = 10^\circ$ and two interferences arrive from $\theta_I = -30^\circ$ and 20°, respectively. In the following, the designed look direction θ_0 is always 0°, which gives an angle estimation error of 10°.

First we perform one simulation based on the RB-FI beamformer. The RV constraint is applied to the range $[-10^\circ, 10^\circ]$. The values of $\sigma = 0.5$, $\delta_l = 0.9$, $\delta_l = 1.1$ and $\chi = 0.4$ are chosen. The resultant beam pattern is shown in Fig. 4, which shows a very good performance in terms of frequency invariant property over the RV angle range, response ripple control and interference suppression.

For RB-FI-WC, the range of RV is $[-10^\circ, 10^\circ]$ and the values of $\varsigma = 0.7$ and $\epsilon = 1.2$ are chosen; for RB-WC, we set $\epsilon = 2.6$. Fig. 5 shows the output SINR versus the input SNR for the RB-FI-WC beamformer, the RB-WC beamformer and the Frost beamformer, obtained by averaging 200 simulation results. Obviously RB-FI-WC and RB-WC are much more effective in coping with the look direction mismatch problem. Moreover, for this case with an estimation error of 10°, the proposed RB-FI-WC provides a better performance than that of RB-WC, especially for high SNRs.

In the next, we study their performances in term of output SINR versus angle estimation error, and the result is shown in Fig. 6(a). It can be seen that the RB-FI-WC beamformer outperforms the RB-WC beamformer when the error is greater than 6°.

As we mentioned in the last section, one potential problem with the RB-WC beamformer is that it may have the frequency response consistency to the mismatched desired signal out of control, leading to an intolerable distortion. The variance of responses at the directions where the mismatched desired signal comes from versus DOA angle is shown in Fig. 6(b), where

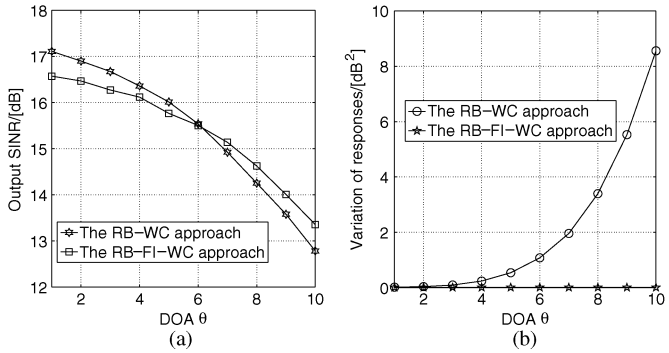

Fig. 6. Comparison of the RB-FI-WC beamformer and the RB-WC beamformer: (a) output SINR versus DOA of the mismatched desired signal with an SNR of 10 dB; (b) variance of responses at the direction where the mismatched desired signal comes from.

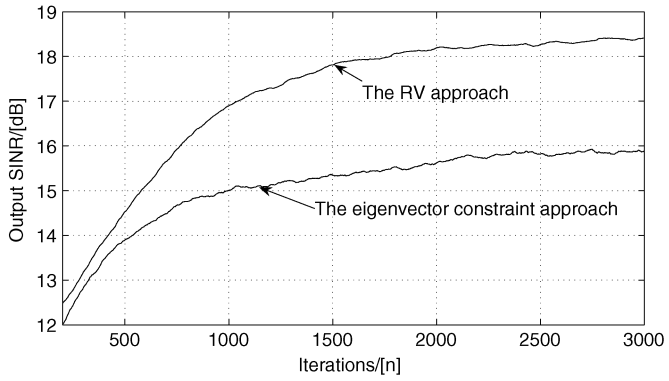

Fig. 7. Convergence of the output SINR for the RV approach in (33) and the eigenvector constraint approach in (22).

the variances for the RB-FI-WC beamformer represent a very good frequency consistency from DOA of 1° to 10°. For the RB-WC beamformer, the variances have a dramatic rise and reach 8.5576 at 10°, causing a too large and intolerable variance of the responses.

Finally we perform some simulations with a larger problem size. The dimensions of the array are increased to $M = 15$ and $J = 40$ and it is assumed that there are four interferences with an SIR of -10 dB coming from -50°, 0° and 30°, 60°, respectively, and one desired signal with an SNR of 10 dB coming from -30°. For the RV approach in (33) and the eigenvector constraint approach in (22), the step size μ is set to 0.000004 and 0.000006, respectively. Based on (69), we have $D_\theta \geq 36$, and therefore we choose $r = 36$. β is set to be 2.5. Fig. 7 shows the learning curves for the output SINR versus the iteration number n, obtained by averaging 200 simulation results. The RV approach again has achieved a better performance. The resultant variance of the magnitude responses at the direction $\theta_0 = -30^\circ$ for the proposed RV approach and the eigenvector constraint approach is 0.0087 and 0.0095, respectively. For RB-FI-WC, the range of RV is $[-40^\circ, -20^\circ]$ and the values of $\varsigma = 2$ and $\epsilon = 1.5$ are chosen; for RB-WC, we set $\epsilon = 3$. The Output SINR versus DOA of the mismatched desired signal is shown in Fig. 8(a), in which the RB-FI-WC beamformer outperforms the RB-WC beamformer when the mismatched desired signal

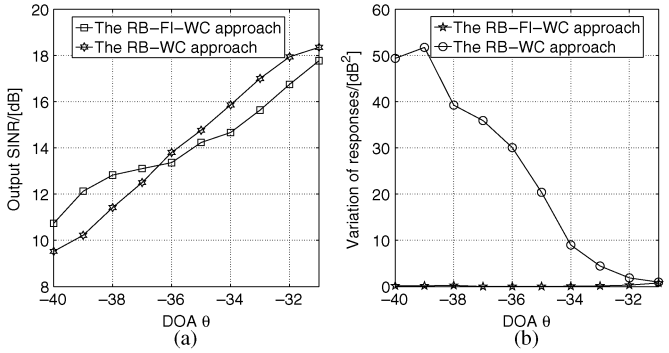

Fig. 8. Comparison of the RB-FI-WC beamformer and the RB-WC beamformer: (a) output SINR versus DOA of the mismatched desired signal with an SNR of 10 dB; (b) variance of responses at the direction where the mismatched desired signal comes from.

comes from between -40° and -37°. The variance of responses at the directions where the mismatched desired signal comes from is shown in Fig. 8(b), where the variances for RB-FI-WC represent a very good frequency consistency from DOA of -40° to -31°. For the RB-WC beamformer, it again causes a too large and intolerable variance of the responses when a large estimation error happens. The variance is much larger than the simulation results shown in Fig. 6(b) with a smaller problem size.

VI. Conclusion

A response variation (RV) element has been introduced to control the frequency invariant property of the adaptive wideband beamformer at the look direction region over the frequency range of interest. By adding it into the cost function of the LCMV beamformer, a new linearly constrained beamformer has been derived with a trade-off between frequency response consistency at the look direction and output power minimization. Due to the increased number of degrees of freedom for interference suppression, compared to the original Frost beamformer and the eigenvector constraint approach, an improved SINR is achieved. In addition, two novel wideband beamformers robust against look direction estimation errors are proposed with their solutions based on the convex optimization technique. One is designed by imposing an constraint on the RV element and simultaneously limiting the magnitude response of the beamformer within a pre-defined angle range at a reference frequency; the other one is obtained by combining the RV element and the worst-case performance optimization method. Compared with the original robust methods, a more efficient and effective control over the beamformer's response at the look direction region has been achieved with an improved overall performance, as shown by our simulations.

Appendix I

In the eigenvector constraint approach, the constraint matrix $\hat{\mathbf{S}}$ is decomposed into the product of three matrices with a singular value decomposition (SVD) operation given by

$$\hat{\mathbf{S}} = \mathbf{U}\Sigma\mathbf{V}^T \tag{62}$$

where Σ is an $MJ \times 2\hat{r}$ diagonal matrix containing the singular values of $\hat{\mathbf{S}}$ in a descending order, $\mathbf{U}$ is an $MJ \times MJ$ unitary matrix and $\mathbf{V}$ is a $2\hat{r} \times 2\hat{r}$ unitary matrix.

To find a rank r approximation matrix $\hat{\mathbf{S}}_r$ to the matrix $\hat{\mathbf{S}}$, we separate matrix $\mathbf{U}$ into two parts as follows:

$$\mathbf{U} = [\mathbf{U}_r, \tilde{\mathbf{U}}_r] \tag{63}$$

where $\mathbf{U}_r$ holds the first r columns of $\mathbf{U}$, and $\tilde{\mathbf{U}}_r$ holds its remaining columns. Matrix $\mathbf{V}$ is split in the same way as

$$\mathbf{V} = [\mathbf{V}_r, \tilde{\mathbf{V}}_r]. \tag{64}$$

Then $\hat{\mathbf{S}}_r$ is given by

$$\hat{\mathbf{S}}_r = \mathbf{U}_r \Sigma_r \mathbf{V}_r^T \tag{65}$$

after which the original constraint formulation changes to

$$\hat{\mathbf{S}}_r \mathbf{w} = \mathbf{V}_r \Sigma_r \mathbf{U}_r^T \mathbf{w} = \hat{\mathbf{g}}. \tag{66}$$

It can be further simplified to

$$\mathbf{U}_r^T \mathbf{w} = \hat{\mathbf{g}}_r \tag{67}$$

with $\hat{\mathbf{g}}_r = \Sigma_r^{-1} \mathbf{V}_r^T \hat{\mathbf{g}}$.

APPENDIX II

The number of constraints in (67) depends on the value of r. A large r leads to a good response consistency at the look direction θ_0, but leaves less number of degrees of freedom for output power minimization. A detailed study has shown that a wideband signal can be represented accurately by [6]

$$D_\theta \geq \left\lceil \frac{B_\theta T_\theta}{\pi} + 1 \right\rceil \tag{68}$$

orthogonal basis functions, where T_θ is the temporal duration for the signal to propagate through the beamformer to the output from the time it first reaches the array, given by $T_\theta = \tau_{M-1} - \tau_0 + (J-1)T_s$; for real-valued bandpass signals within the frequency range $[\omega_{min}, \omega_{max}]$, $B_\theta = \omega_{max} - \omega_{min}$, and $\lceil \bullet \rceil$ is the ceiling function rounding its element to the next integer towards infinity [6]. Then as a guideline, r is chosen to be D_θ to span the constraint space effectively. Based on the normalized angular frequency Ω and $\mu = d/cT_s$, (68) changes to

$$D_\theta \geq \left\lceil \frac{(\Omega_{max} - \Omega_{min})\left[(M-1)\mu \left|sin(\theta)\right| + (J-1)\right]}{\pi} + 1 \right\rceil \tag{69}$$

where the frequency range of interest $\Omega_I = [\Omega_{min}, \Omega_{max}]$.

REFERENCES

[1] W. Liu and S. Weiss, *Wideband Beamforming: Concepts and Techniques*. Chichester, U.K.: Wiley, 2010.

[2] E. W. Vook and R. T. Compton, Jr., "Bandwidth performance of linear adaptive arrays with tapped delay-line processing," *IEEE Trans. Aerosp. Electron. Syst.*, vol. 28, no. 3, pp. 901–908, July 1992.

[3] N. Lin, W. Liu, and R. J. Langley, "Performance analysis of an adaptive broadband beamformer based on a two-element linear array with sensor delay-line processing," *Signal Processing*, vol. 90, pp. 269–281, Jan. 2010.

[4] O. L. Frost, III, "An algorithm for linearly constrained adaptive array processing," *Proc. IEEE*, vol. 60, no. 8, pp. 926–935, Aug. 1972.

[5] B. D. Van Veen and K. M. Buckley, "Beamforming: A versatile approach to spatial filtering," *IEEE Acoust., Speech, Signal Processing Mag.*, vol. 5, no. 2, pp. 4–24, April 1988.

[6] K. M. Buckley, "Spatial/spectral filtering with linearly constrained minimum variance beamformers," *IEEE Trans. Acoust., Speech, Signal Processing*, vol. ASSP-35, no. 3, pp. 249–266, Mar. 1987.

[7] M. S. Brandstein and D. Ward, Eds., *Microphone Arrays: Signal Processing Techniques and Applications*. Berlin, Germany: Springer, 2001.

[8] J. Li and P. Stoica, Eds., *Robust Adaptive Beamforming*. Hoboken, NJ: Wiley, 2005.

[9] M. H. Er and A. Cantoni, "Derivative constraints for broadband element space antenna array processors," *IEEE Trans. Antennas Propag.*, vol. AP-31, no. 6, pp. 1378–1393, Dec. 1983.

[10] K. M. Buckley and L. J. Griffith, "An adaptive generalized sidelobe canceller with derivative constraints," *IEEE Trans. Antennas Propag.*, vol. 34, no. 3, pp. 311–319, Mar. 1986.

[11] K. C. Huarng and C. C. Yeh, "Performance analysis of derivative constraint adaptive arrays with pointing errors," *IEEE Trans. Antennas Propag.*, vol. 40, pp. 975–981, Aug. 1992.

[12] B. D. Carlson, "Covariance matrix estimation errors and diagonal loading in adaptive arrays," *IEEE Trans. Aerosp. Electron. Syst.*, vol. 24, pp. 397–401, Jul. 1988.

[13] B. D. Van Veen, "Minimum variance beamforming with soft response constraints," *IEEE Trans. Signal Processing*, vol. 39, no. 9, pp. 1964–1972, Sep. 1991.

[14] M. H. Er, "On the limiting solution of quadratically constrained broadband beam formers," *IEEE Trans. Signal Processing*, vol. 43, no. 1, pp. 418–419, Jan. 1993.

[15] Z. L. Yu, W. Ser, M. H. Er, Z. H. Gu, and Y. Q. Li, "Robust adaptive beamformers based on worst-case optimization and constraints on magnitude response," *IEEE Trans. Signal Processing*, vol. 57, pp. 2615–2628, Jul. 2009.

[16] S. A. Vorobyov, A. B. Gershman, and Z.-Q. Luo, "Robust adaptive beamforming using worst-case performance optimization: A solution to the signal mismatch problem," *IEEE Trans. Acoust., Speech, Signal Processing*, vol. 51, pp. 313–324, Feb. 2003.

[17] M. Rubsamen and A. B. Gershman, "Robust presteered broadband beamforming based on worst-case performance optimization," in *Proc. IEEE Workshop on Sensor Array and Multichannel Signal Processing*, Darmstadt, Germany, Jul. 2008, pp. 340–344.

[18] H. Duan, B. P. Ng, C. M. See, and J. Fang, "Applications of the SRV constraint in broadband pattern synthesis," *Signal Processing*, vol. 88, pp. 1035–1045, Apr. 2008.

[19] Y. Zhao, W. Liu, and R. J. Langley, "Subband design of fixed wideband beamformers based on the least squares approach," *Signal Processing*, vol. 91, pp. 1060–1065, Apr. 2011.

[20] Y. Zhao, W. Liu, and R. J. Langley, "An application of the least squares approach to fixed beamformer design with frequency invariant constraints," *IET Signal Processing*, vol. 5, 2011.

[21] D. P. Scholnik and J. O. Coleman, "Formulating wideband array-pattern optimizations," in *Proc. IEEE Int. Conf. on Phased Array Systems and Technology*, Dana Point, CA, May 2000, pp. 489–492.

[22] J. K. Sturm, "Using SeDuMi 1.02, a MATLAB toolbox for optimization over symmetric cones," *Optimiz. Meth. Software*, vol. 11–12, pp. 625–653, Aug. 1999.

[23] M. Lobo, L. Vandenberghe, S. Boyd, and H. Lebret, "Applications of second-order cone programming," *Linear Alg. Its Applicat.*, vol. 284, pp. 193–228, Nov. 1998.

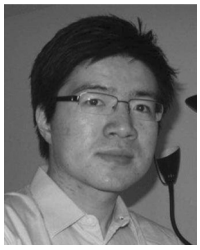

Yong Zhao was born in Liaoning, China, in May 1983. He received the B.Eng. degree in communication engineering from Tianjin University, China, in 2006 and the M.Sc. degree in communications and signal processing from Imperial College London, U.K., in 2007. Since December 2007, he has been working toward the Ph.D. degree at the University of Sheffield, Sheffield, U.K.

His research interests include array signal processing and multirate systems.

Wei Liu (S'01–M'04–SM'04) was born in Hebei, China, in January 1974. He received the B.Sc. degree in space physics (minor in electronics) and the L.L.B. degree in Intellectual property law both from Peking University, China, in 1996 and 1997, respectively, the M.Phil. degree from the University of Hong Kong, in 2001, and the Ph.D. degree from the University of Southampton, Southampton, U.K., in 2003.

He then worked as a Postdoctoral Researcher in the Communications Research Group, School of Electronics and Computer Science, University of Southampton, and later in the Communications and Signal Processing Group, Department of Electrical and Electronic Engineering, Imperial College London, U.K. Since September 2005, he has been with the Communications Research Group, Department of Electronic and Electrical Engineering, University of Sheffield, Sheffield, U.K., as a Lecturer. His research interests are mainly in array signal processing, blind source separation/extraction, and multirate signal processing. He has now authored and coauthored about 90 journal and conference publications, and a monograph about wideband beamforming, *Wideband Beamforming: Concepts and Techniques* (Wiley, March 2010).

Richard J. Langley (M'85) received the B.Sc. and Ph.D. degrees from the University of Kent, Kent, U.K.

After spending some time working on communications satellites at Marconi Space Systems in the 1970s he became a Lecturer at the University of Kent in 1979. He was promoted to a personal Chair in Antenna Systems in 1994. In 1997 he founded the European Technology Centre for Harada Industries Japan, the world's largest supplier of automotive antennas. The center researches and develops advanced hidden antenna systems for the global automotive market including radio, telephone and navigation systems. After successfully building up the technology and business he rejoined academic life in 2003. He is currently Head of the Communications Research Group, University of Sheffield, Sheffield, U.K. His main research is in the fields of automotive antennas, propagation in the built environment, frequency selective surfaces, electromagnetic band gap materials and applications, multi-function antenna systems and reconfigurable antennas. He has published over 250 papers in international journals and conferences

Prof. Langley was Honorary Editor of the *Inst. Elect. Eng. Proceedings—Microwaves, Antennas and Propagation* from 1995 to 2003. In 2009, he initiated the setting up of the Wireless Friendly Building Forum to address the problems of wireless signal propagation in buildings and the built environment. He is currently Chair of the IET Antennas and Propagation Professional Network.